On the Construction of Nested Explicit Runge–Kutta Methods via Null Rules

M.R. Belardo[+], F. Calabrò[*], G. Izzo[*], E. Messina[*], and V. Veneroso[#],

+ Scuola Superiore Meridionale, E-mail: mariaroberta.belardo-ssm@unina.it

** Dipartimento di Matematica e Applicazioni "R. Caccioppoli", Università di Napoli "Federico II", E-mail: {francesco.calabro, giuseppe.izzo, eleonora.messina } @unina.it*

 # Dipartimento di Matematica e Applicazioni "R. Caccioppoli", Università di Napoli "Federico II", E-mail: venerosov@gmail.com

1 Introduction

This work is based on the simple yet crucial observation that the difference between the weights of two nested Explicit Runge–Kutta (ERK) methods—the usual vector used for error estimation—constitutes a null rule with respect to the exactness equations. In this note, we aim to exploit this fact by constructing nested RK methods through the addition of a null rule to the weight vector of an existing RK method. This approach makes it possible to obtain additional (lower-order) methods that estimate the solution solely by computing linear combinations of stages already evaluated once.

This availability can be exploited in different ways: to design criteria for step-size adaptation as is typically done in nested methods, but also for stiffness detection [8–10,15]. In all cases, the construction offers an alternative method—with no significant additional computational cost—that has a lower convergence order but, as we shall see, can achieve a larger stability region.

Null rules were first introduced in [11] in the context of numerical quadrature, where they are employed in automatic quadrature algorithms to estimate local error. For a review on the subject in the framework of numerical quadrature, as well as for applications of such rules in the detection of reduced regularity, we refer to [1,3,4]. Nested ERK methods are, on the one hand, a well-established class of reference methods and, on the other hand, still a very active research area. Without aiming at completeness, we refer to [5,6,12–14,16–20] for some recent progress in the construction of new methods.

In this paper, we present a general procedure for the construction of nested

rules, comment on certain limitations, and discuss the choice of free parameters with respect to the absolute stability region of the new methods. To make the construction explicit, we finally provide some examples. In particular: we derive an embedding of order 1 for the ERK Midpoint, we derive a nested rule of order 2 for the widely used fourth-order explicit RK method with nodes $[0, 1/2, 1/2, 1]$; we present the construction of nested rules of orders 4 and 3 for the Dormand & Prince 5–4 RK method; and we introduce nested methods for the ERK schemes recently proposed in [2].

2 Preliminary results and remarks

Explicit RK methods are defined by the triple (A, b, c), where we refer to c as the nodes and b as the weights, and can be represented by the Butcher tableau

$$\begin{array}{c|c} \mathbf{c} & \mathbf{A} \\ \hline & \mathbf{b}^T \end{array} = \begin{array}{c|cccc} c_1 & & & & \\ c_2 & a_{21} & & & \\ c_3 & a_{31} & a_{32} & & \\ \vdots & \vdots & \vdots & \ddots & \\ c_s & a_{s,1} & a_{s,2} & \cdots & a_{s,s-1} \\ \hline & b_1 & b_2 & \cdots & b_{s-1} \quad b_s \end{array}$$

We assume that the row-sum condition holds, that is $\mathbf{Ae} = \mathbf{c}$. Order Conditions, in matrix form, for Runge-Kutta methods up to order $p = 4$ are reported in Table 1, where vector power such as $\mathbf{c}^2$ and $\mathbf{c}^3$ stands for componentwise power, and $\mathbf{D_c} = diag(\mathbf{c})$. As is well known, for $p = 5$ there are 17 order conditions, and their number grows exponentially with the order p, making a direct use of full order conditions increasingly impractical beyond moderate orders.

Order	**Condition**	**Order**	**Condition**
$p = 1$	1) $\mathbf{b}^\top \mathbf{e} = 1$	$p = 4$	5) $\mathbf{b}^\top \mathbf{c}^3 = \frac{1}{4}$
$p = 2$	2) $\mathbf{b}^\top \mathbf{c} = \frac{1}{2}$		6) $\mathbf{b}^\top (\mathbf{D_c}\, \mathbf{A}\, \mathbf{c}) = \frac{1}{8}$
$p = 3$	3) $\mathbf{b}^\top \mathbf{c}^2 = \frac{1}{3}$		7) $\mathbf{b}^\top \mathbf{A}\, \mathbf{c}^2 = \frac{1}{12}$
	4) $\mathbf{b}^\top \mathbf{A}\, \mathbf{c} = \frac{1}{6}$		8) $\mathbf{b}^\top \mathbf{A}\, \mathbf{A}\, \mathbf{c} = \frac{1}{24}$

Table 1
Order conditions for Runge–Kutta methods up to order $p = 4$.

If A and c are fixed while b is to be determined, these conditions can be regarded as a set of linear equations in the variables (b_i). To make the con-

struction explicit, let us fix b as a solution of the full system of $n_p = 8$ equations listed in the table, so that the corresponding Runge–Kutta method (A, b, c) attains at least order 4. Now, let N denote a solution of the linear system, with homogeneous right-hand side—what is commonly referred to in the literature as a *null rule*. It can be noticed that $b + N$ will also define a weight vector giving a method $(A, b + N, c)$ of order $p = 4$. Based on this observation, one can construct nested Runge–Kutta schemes starting from known methods. This construction is not always possible, as it is subject to the well-known Butcher barriers and the uniqueness properties of Runge–Kutta schemes, and is related to the rank of the matrices involved. Moreover, any method of the form $(A, b + kN, c)$ with $k \in \mathbb{R}$ will also preserve the order of $b + N$.

3 Embeddings via Null Rules of Order Conditions

Now we discuss the construction of the null rules, focusing on the exactness achieved and on the role of k. We start from an s-stage order q explicit Runge–Kutta method given by the triple (A, b, c). Denote by $\Phi_p \in \mathbb{R}^{n_p \times s}$, $\Phi_p \equiv \Phi_p(A, c)$, the order-condition matrix up to order $p \leq q$ built from the linear order conditions in Table 1, so that the order constraints up to p can be written compactly as

$$\Phi_p \, b \;=\; r_p, \tag{1}$$

where n_p is the number of conditions, $r_p \in \mathbb{R}^{n_p}$ collects the corresponding right-hand sides. The desired null rules of order p are the nonzero vectors $N \in \ker\left(\Phi_p\right)$. If $\dim\ker(\Phi_p) = d \geq 1$, we denote by

$$Z_p \;=\; \Big[\, Z_p(:,1) \;\; Z_p(:,2) \;\; \cdots \;\; Z_p(:,d) \,\Big] \in \mathbb{R}^{s \times d}$$

an orthonormal basis of $\ker\left(\Phi_p\right)$. Given a base method (A, b, c) satisfying (1), every vector in the affine family

$$b^{(k)} \;=\; b \;+\; k\, Z_p(:,j), \qquad k \in \mathbb{R},\; j \in \{1, \ldots, d\}, \tag{2}$$

also satisfies $\Phi_p \, {b^{(k)}}^{\top} = r_p$, i.e., $b^{(k)}$ preserves all order conditions up to p while reusing the same stages. We refer to the j-th column $Z_p(:,j)$ for the order p as *Null Rule*$_p$ $\#j$. For each embedded family we define the linear stability function

$$R(z) = \det\left(I - zA + z\,\mathbf{e}\,{b^{(k)}}^{\top}\right),$$

and the stability region of the method as

$$S = \{z \in \mathbb{C} \,:\, |R(z)| \leq 1\}.$$

In order to study S as a function of k, we choose as indicator the maximum real stability boundary and determine k so that for an interval $[-\rho, 0]$, with $\rho > 0$

as large as possible, the following condition is valid: $R(z) \leq 1$, $z \in [-\rho, 0]$.

Remarks

- The stability regions vary continuously with k, starting from the case $k = 0$ which corresponds to the original (non-nested) method. Hence, one can tune k to achieve a specific objective: for example, to make the region resemble a desired shape or to maximize ρ.
- In general we look for *Null Rule*$_p$, $p = q, \ldots, 1$ so to nest the original method with equal and lower order methods.
- It is worth noticing that explicit Runge-Kutta methods with four stages and order four cannot be nested while preserving order $p = 3$ (see [7]). This can be motivated in the null rule framework by observing that, for any 4–stage, order–4 ERK, the order–three condition matrix Φ_3 is full–rank, i.e., $\ker \Phi_3 = \{0\}$, so no nontrivial null rule exists.

4 Some constructed rules

In this section, we illustrate how the construction is applied to several ERK schemes, namely the explicit Midpoint method, the classical RK4 method, the Dormand–Prince 5(4) pair, and the five-stage order-3 scheme of [2]. We display results only for $k > 0$: whenever the maximizer of $\rho(k)$ occurs at a negative value, we reverse the sign of the chosen null rule and reparameterize the family of embedded weights. This sign change leaves the embedded methods unchanged and simply yields a clearer visualization.

Runge-Kutta Midpoint We consider the two–stage midpoint method. For this scheme the only admissible embedding preserves order $p = 1$, i.e. corresponding to the *Null Rule*$_1 \equiv \frac{1}{\sqrt{2}}(1, -1)^\top$. The weights are nonnegative for $k \in [0, \sqrt{2}]$. Figure 1b reports the maximum real stability interval $\rho(k)$ versus k, where we notice that the maximum real stability interval is 7, while the original method has $\rho = 2$ as it can be seen in the plot at $k = 0$. In Figure 1 we report the results for the 1st order embedding and embedded tableau at $k = 1$, where ρ attains its maximum. For this method, no order-two embedding exists, because the order-two condition matrix Φ_2 has full rank, hence no null rule is available.

Runge-Kutta 4 We consider the standard four–stage Runge–Kutta method. An order-four embedding for this rule is not avaible since Φ_4 has full rank and,

0		
$\frac{1}{2}$	$\frac{1}{2}$	
	0	1
	$\frac{1}{\sqrt{2}}$	$1-\frac{1}{\sqrt{2}}$

(a) Embedded tableau with first–order embedding ($k = 1$).

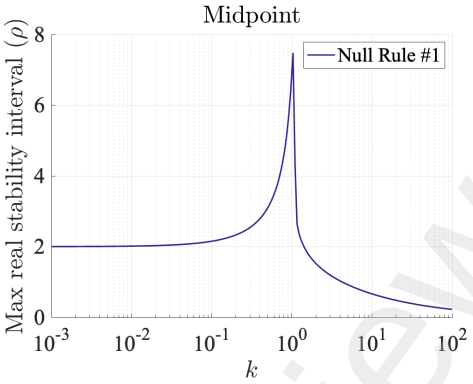

(b) Maximum real-axis stability interval $\rho(k)$ for $b^{(k)} = b + k\,N^\top$.

Fig. 1. Midpoint method: embedded tableau and stability interval $\rho(k)$.

0				
$\frac{1}{2}$	$\frac{1}{2}$			
$\frac{1}{2}$	0	$\frac{1}{2}$		
1	0	0	1	
	$\frac{1}{6}$	$\frac{1}{3}$	$\frac{1}{3}$	$\frac{1}{6}$
	$\frac{667}{6215}$	$\frac{330}{1261}$	$\frac{1007}{1923}$	$\frac{667}{6215}$

(a) Embedded tableau (Null Rule #1).

0				
$\frac{1}{2}$	$\frac{1}{2}$			
$\frac{1}{2}$	0	$\frac{1}{2}$		
1	0	0	1	
	$\frac{1}{6}$	$\frac{1}{3}$	$\frac{1}{3}$	$\frac{1}{6}$
	$\frac{543}{1696}$	$\frac{917}{2987}$	$\frac{223}{3387}$	$\frac{543}{1696}$

(b) Embedded tableau (Null Rule #2).

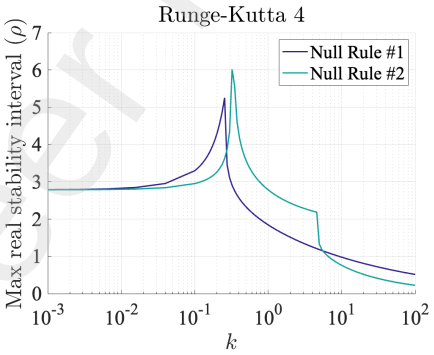

(c) Maximum real-axis stability interval $\rho(k)$.

Fig. 2. Runge-Kutta 4: two order-2 embedded methods (left, center) and their stability interval $\rho(k)$ with their independent choices that give order 2 (right).

as discussed in the introduction, no embedded construction preserving $p = 3$ is available for this scheme. Instead, the matrix Φ_2 built from the order conditions in Table 1 up to $p = 2$ has a null space of dimension 2, yielding two independent directions (*Null Rule*$_2$#1 and *Null Rule*$_2$#2), see Figure 2c. In Figures 2a, 2b we report, for each direction, a positive–weights embedded tableau at a value of k where $\rho(k)$ is maximal.

Runge-Kutta DOPRI 5(4) We consider the seven–stage Dormand–Prince pair with principal weights b delivering order 5 and the standard embedded weights $\hat{b}$ delivering order 4. Restricting to the order–four conditions, the associated matrix Φ_4 has a one–dimensional null space, i.e., $\dim\ker\Phi_4 = 1$. Consequently, every order–four embedding compatible with the fixed (A, c) can be written as the one–parameter affine family $b^{(k)} = b + k\,Z_4$, $Z_4 \in \ker\Phi_4 \setminus \{0\}$,

0							
$\frac{1}{5}$	$\frac{1}{5}$						
$\frac{3}{10}$	$\frac{3}{40}$	$\frac{9}{40}$					
$\frac{4}{5}$	$\frac{44}{45}$	$-\frac{56}{15}$	$\frac{32}{9}$				
$\frac{8}{9}$	$\frac{19372}{6561}$	$-\frac{25360}{2187}$	$\frac{64448}{6561}$	$-\frac{212}{729}$			
1	$\frac{9017}{3168}$	$-\frac{355}{33}$	$\frac{46732}{5247}$	$\frac{49}{176}$	$-\frac{5103}{18656}$		
1	$\frac{35}{384}$	0	$\frac{500}{1113}$	$\frac{125}{192}$	$-\frac{2187}{6784}$	$\frac{11}{84}$	
	$\frac{35}{384}$	0	$\frac{500}{1113}$	$\frac{125}{192}$	$-\frac{2187}{6784}$	$\frac{11}{84}$	0
	$\frac{85}{949}$	0	$\frac{311}{684}$	$\frac{422}{699}$	$-\frac{309}{1201}$	$\frac{59}{763}$	$\frac{35}{1094}$

Fig. 3. Butcher tableau for the DOPRI5(4) with an order-4 embedded rule.

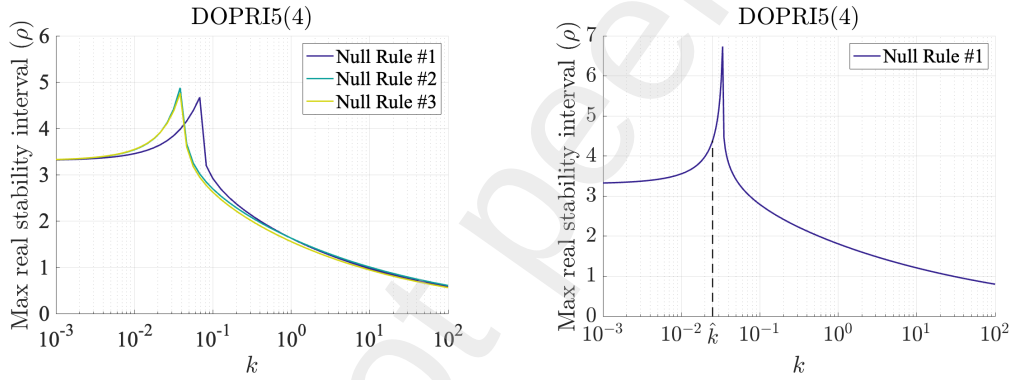

(a) Order 3 Null Rules. (b) Order 4 Null Rule.

Fig. 4. Maximum real-axis stability interval $\rho(k)$ for Dormand–Prince embedded families (left: $p = 3$, right: $p = 4$).

so that $\hat{b} = b + \hat{k}\, Z_4$.

More generally, the null–rule framework can be adapted even when a built–in embedding already exists since lower–order embeddings solve the reduced linear order conditions coming from Φ_p. Hence, varying k provides a way to scan that affine family and identify the element delivering a wider stability regions. Along this family, the real stability interval attains its maximum at a value $k^\star > \hat{k}$. So the corresponding method $b^\star$ is an order–four embedded rule different from the standard Dormand–Prince $\hat{b}$. Finally, we also construct order–three embeddings by solving the order–three linear conditions and extracting a basis of $\ker \Phi_3$, shown in Figure 4a.

0					
$\frac{3}{11}$	$\frac{3}{11}$				
$\frac{15}{19}$	$\frac{285645}{493487}$	$\frac{103950}{493487}$			
$\frac{5}{6}$	$\frac{3075805}{5314896}$	$\frac{1353275}{5314896}$			
1	$\frac{196687}{177710}$	$-\frac{129383023}{426077496}$	$\frac{48013}{42120}$	$-\frac{2268}{2405}$	
	$\frac{5626}{4725}$	$-\frac{25289}{13608}$	$\frac{569297}{340200}$	$\frac{324}{175}$	$-\frac{13}{7}$
	$\frac{249}{249499}$	$\frac{809}{1397}$	$\frac{485}{2642}$	$\frac{305}{1297}$	$\frac{33}{28133}$

(a) Butcher tableau with an order-2 embedded rule.

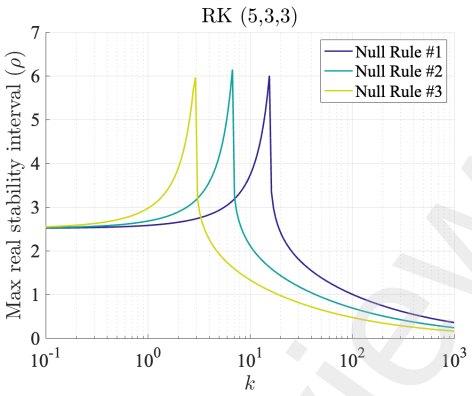

(b) Maximum real-axis stability interval $\rho(k)$ for the RK (5,3,3) embedded family of order 2.

Fig. 5. RK (5,3,3): embedded tableau and corresponding stability plot.

Runge-Kutta (5,3,3) We consider the 3rd order–5 stage ERK introduced in [2] to alleviate order reduction typically observed in initial-boundary value problem with time-dependent boundary conditions. Assembling the order–three matrix shows that $\dim\ker(\Phi_3) = 1$. A generator of this one-dimensional null space is

$$Z_3^\top = [\tfrac{-49}{531}, \tfrac{143}{695}, \tfrac{-739}{976}, \tfrac{2119}{3461}, \tfrac{66}{2099}]$$

consequently, all order–three admissible weight vectors for this method lies in the one–parameter affine family determined by Z_3.
Restricting the order conditions in Table 1 to $p = 2$ yields a matrix Φ_2 whose null space has dimension 3, thus providing three independent directions (see Figure 5b) for constructing embedded families that preserve $p = 2$. Figure 5b reports the maximum real stability interval $\rho(k)$ versus k for all three families. Among them, only the third family admits nonnegative weights over an empty range of k; for this case we also report a positive–weights embedded tableau at a value of k where $\rho(k)$ is maximal.

Acknowledgements

Authors are partially supported by INdAM, through GNCS research projects. This support is gratefully acknowledged.
GI and FC were partially supported by PRIN 2022 2022N3ZNAX "Numerical Optimization with Adaptive Accuracy and Applications to Machine Learning". EM was partially supported by PRIN 2022XZSAFN "Anomalous Phenomena on Regular and Irregular Domains: Approximating Complexity for the Applied Sciences".

References

[1] J. Berntsen and T.O. Espelid, *Error estimation in automatic quadrature routines*, ACM Transactions on Mathematical Software **17** (1991), no. 2, 233–253.

[2] A. Biswas, D. Ketcheson, S. Roberts, B. Seibold, and D. Shirokoff, *Explicit Runge–Kutta methods that alleviate order reduction*, SIAM J. on Numerical Analysis **63** (2025), no. 4, 1398–1426.

[3] C. Bracco, F. Calabrò, and C. Giannelli, *Discontinuity detection by null rules for adaptive surface reconstruction*, J. of Scientific Computing **97** (2023), no. 2, 37.

[4] F. Calabrò, D. Bravo, C. Carissimo, E. Di Fazio, A. Di Pasquale, A. Eldray, C. Fabrizi, J. Gerges, S. Palazzo, and J. Wassef, *Null rules for the detection of lower regularity of functions*, J. of Computational and Applied Mathematics **361** (2019), 547–553.

[5] E.M. Constantinescu, *Generalizing global error estimation for ordinary differential equations by using coupled time-stepping methods*, J. of Computational and Applied Mathematics **332** (2018), 140–158.

[6] V.M. Deshpande, R. Bhattacharya, and D.A. Donzis, *A unified framework to generate optimized compact finite difference schemes*, J. of Computational Physics **432** (2021), 110157.

[7] Ernst Hairer, Gerhard Wanner, and Syvert P Nørsett, *Solving ordinary differential equations i: Nonstiff problems*, Springer, 1993.

[8] G-Y. Kulikov, *Nested implicit Runge–Kutta pairs of Gauss and Lobatto types with local and global error controls for stiff ordinary differential equations*, Computational Mathematics and Mathematical Physics **60** (2020), no. 7, 1134–1154.

[9] G-Y. Kulikov and R. Weiner, *A singly diagonally implicit two-step peer triple with global error control for stiff ordinary differential equations*, SIAM J. on Scientific Computing **37** (2015), no. 3, A1593–A1613.

[10] ———, *Doubly quasi-consistent fixed-stepsize numerical integration of stiff ordinary differential equations with implicit two-step peer methods*, J. of Computational and Applied Mathematics **340** (2018), 256–275.

[11] J.N. Lyness, *Symmetric integration rules for hypercubes. III. construction of integration rules using null rules*, Mathematics of Computation **19** (1965), no. 92, 625–637.

[12] J. Muñoz-Matute, D. Pardo, V.M. Calo, and E. Alberdi, *Variational formulations for explicit Runge–Kutta methods*, Finite Elements in Analysis and Design **165** (2019), 77–93.

[13] H. Ranocha, L. Dalcin, M. Parsani, and D. Ketcheson, *Optimized Runge–Kutta methods with automatic step size control for compressible computational fluid dynamics*, Communications on Applied Mathematics and Computation **4** (2022), no. 4, 1191–1228.

[14] H. Ranocha, M. Sayyari, L. Dalcin, M. Parsani, and D. Ketcheson, *Relaxation Runge–Kutta methods: Fully discrete explicit entropy-stable schemes for the compressible euler and navier–stokes equations*, SIAM J. on Scientific Computing **42** (2020), no. 2, A612–A638.

[15] M. Sofroniou and G. Spaletta, *Construction of explicit Runge–Kutta pairs with stiffness detection*, Mathematical and Computer Modeling **40** (2004), no. 11-12, 1157–1169.

[16] B.C. Vermeire, *Paired explicit Runge–Kutta schemes for stiff systems of equations*, J. of Computational Physics **393** (2019), 465–483.

[17] B.C. Vermeire, N.A. Loppi, and P.E. Vincent, *Optimal embedded pair Runge–Kutta schemes for pseudo-time stepping*, J. of Computational Physics **415** (2020), 109499.

[18] B.C. Vermeire and S.H. Nasab, *Accelerated implicit-explicit Runge–Kutta schemes for locally stiff systems*, J. of Computational Physics **429** (2021), 110022.

[19] R. Weiner, G-Y. Kulikov, S. Beck, and J. Bruder, *New third-and fourth-order singly diagonally implicit two-step peer triples with local and global error controls for solving stiff ordinary differential equations*, J. of Computational and Applied Mathematics **316** (2017), 380–391.

[20] H. Zhang, X. Qian, J. Yan, and S. Song, *Highly efficient invariant-conserving explicit Runge–Kutta schemes for nonlinear hamiltonian differential equations*, J. of Computational Physics **418** (2020), 109598.